VOL. 55 NO. 2, FEB. 2002 THE JOURNAL OF ANTIBIOTICS pp. 204 — 207

NOTES

Trienomycin G, a New Inhibitor of Nitric Oxide Production in Microglia Cells, from *Streptomyces* sp. 91614

WON-GON KIM, NAN-KYU SONG and ICK-DONG YOO*

Korea Research Institute of Bioscience and Biotechnology, P. O. Box 115, Yusong, Taejon 305-600, Korea

(Received for publication August 16, 2001)

Nitric oxide (NO) plays an important role in the physiology and pathophysiology of the central nervous, cardiovascular, and immune systems[1~3]. NO is produced by the oxidation of L-arginine to L-citrulline by one of three isoenzymes of nitric oxide synthase (NOS): neuronal (nNOS), endothelial (eNOS), and inducible (iNOS)[4,5]. iNOS produces higher levels of NO which plays a role in host defence mechanisms but is also implicated in the pathogenesis of various inflammatory diseases such as septic shock, rheumatoid arthritis, inflammatory bowel disease, and neurodegenerative diseases[6~8]. Activation of microglia is a histopathological hallmark of neurodegenerative diseases including post-ischemic stroke, Alzheimer's disease, Parkinson's disease, multiple sclerosis, and the AIDS dementia complex[9~11]. Microglia activation

Fig. 1. Structures of trienomycin G (**1**) and trienomycin A (**2**).

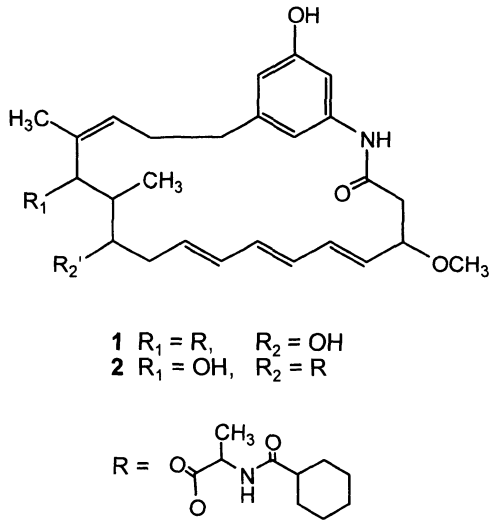

Table 1. Physico-chemical property of **1**.

Appearance	white powder
$[\alpha]_D$	+53 (*c* 0.6, MeOH)
ESI-MS (*m/z*)	623 $(M+H)^+$
HRESI-MS (*m/z*)	
found	623.3794
calcd.	623.3696
Molecular formula	$C_{36}H_{50}N_2O_7$
UV λ_{max} nm (log ε)(MeOH)	250(4.16), 262(4.17), 271(4.24), 283(4.13)
IR (KBr) γcm^{-1}	3312, 2927, 1730, 1654, 1549, 1449, 1096
TLC (Rf)[a]	0.32
HPLC (R_t)[b] (minute)	20

[a] Silica gel TLC (Kieselgel $60F_{254}$, Merck); solvent, $CHCl_3$-MeOH (10:1).
[b] Column, Cosmosil C_{18} (4.6 x 150 mm); solvent, CH_3CN-H_2O (50:50); flow rate, 0.5 ml/min; UV absorbance at 280 nm.

* Corresponding author: idyoo@mail.kribb.re.kr

is believed to contribute to neurodegenerative processes through the release of various pro-inflammatory cytokines and the overproduction of NO[12~14]. In this respect, an inhibitor of NO production in microglia cells may be a potential therapeutic agent for intervention of various inflammatory and neurodegenerative diseases[15,16]. Vineomycin C has been isolated as the inhibitor of iNOS from microbial metabolites[17]. In the course of our screening for inhibitors of NO production in BV-2 microglia cells, we isolated a new potent compound named trienomycin G (**1**) from a fermentation broth of *Streptomyces* sp. 91614 (Fig. 1). In addition, the related known compound, trienomycin A[18] (**2**), was also detected in the same culture broth. We report here the fermentation, isolation, physico-chemical properties, structure determination, and biological activities of **1**.

The producing strain G91614 was isolated from a soil sample collected in Taejon-city, Chungcheongnam-do, Korea and assigned to the *Streptomyces* sp. Fermentation was carried out in 1-liter Erlenmeyer flasks containing soluble starch 1%, glucose 2%, soybean meal 2.5%, beef extract 0.1%, yeast extract 0.4%, NaCl 0.2%, K_2HPO_4 0.025%, and $CaCO_3$ 0.2% (adjusted to pH 7.2 before sterilization). A piece of strain G91614 from a mature plate culture was inoculated into a 500 ml Erlenmeyer flask containing 80 ml of sterile seed liquid medium with the above composition and cultured on a rotary shaker (150 rpm) at 28°C for 3 days. For the production of **1**, 5 ml of the seed culture was transferred into one-liter Erlenmeyer flasks (35 flasks) containing 150 ml of the above medium, and cultivated for 6 days using the same conditions. The culture supernatant obtained from the culture broth (5 liters) was extracted with an equal volume of EtOAc three times and the EtOAc layer was concentrated *in vacuo*. The resultant residue was subjected to SiO_2 (Merck Art No. 7734.9025) column chromatography followed by elution with $CHCl_3$ - MeOH (15 : 1). The active fractions were pooled and concentrated *in vacuo* to give an oily residue. The residue was applied again to a Sephadex LH-20 and then eluted with MeOH. Active fraction dissolved in MeOH was further purified by reverse phase HPLC column (20×250 mm, YMC C_{18}) chromatography with a photodiode array detector. The column was eluted with CH_3CN - H_2O (60 : 40) at a flow rate of 7 ml/minute to afford **2** (5.6 mg) and **1** (3.3 mg) at a retention time of 16 and 21 minutes, respectively, as white powder.

The physico-chemical properties of **1** are summarized in Table 1. It is soluble in methanol, dimethylsulfoxide and $CHCl_3$, and insoluble in water, ether and *n*-hexane. After TLC on silica gel 60 F_{254} (Merck) with $CHCl_3$ - MeOH (10 : 1), **1** showed an Rf value of 0.32 whereas **2** had an Rf value of 0.34. The UV spectrum showed absorption maxima at 250, 262, 271, and 283 nm which was almost same as that of **2**. In the IR spectrum, the absorption bands attributable to an triene (1096 cm^{-1}), an amide (1654 cm^{-1}), an ester (1730 cm^{-1}), and NH or OH (3312 cm^{-1}) were observed.

The molecular formula of **1** was determined to be $C_{36}H_{50}N_2O_7$ on the basis of high resolution ESI-MS [$(M+H)^+$, *m/z* 623.3794 (−9.8 mmu error)] in combination with ^1H and ^{13}C NMR data. The ^1H NMR and ^{13}C NMR

Table 2. ^1H and ^{13}C NMR spectral data of **1** and **2**.

No.	**1**		**2**	
	δ_H	δ_C	δ_H	δ_C
1		168.4 s		168.5 s
2	2.80, 2.49	44.0 t	2.61, 2.75	43.5 t
3	4.09	79.1 d	4.12	78.5 d
4	5.58	130.7 d	5.62	130.6 d
5	6.28	134.5 d	6.25	133.5 d
6	6.12	128.7 d	6.00	129.3 d
7	6.14	134.8 d	6.00	134.1 d
8	6.04	132.7 d	6.05	133.4 d
9	5.84	131.2 d	5.57	129.4 d
10	2.53, 2.27	36.4 t	2.52, 2.33	33.1 t
11	3.63	71.0 d	4.93	75.5 d
12	1.86	40.5 d	1.86	39.6 d
13	5.92	75.0 d	4.62	68.4 d
14		134.0 s		138.6 s
15	5.23	126.4 d	5.20	124.7 d
16	2.02, 2.41	29.0 t	2.20, 1.97	29.3 t
17	2.55, 2.39	35.8 t	2.46	36.2 t
18		143.7 s		144.1 s
19	6.24	111.1 d	6.20	110.8 d
20		138.2 s		138.4 s
21	7.36	105.6 d	7.50	105.7 d
22		157.0 s		157.2 s
23	6.45	112.0 d	6.50	111.9 d
24	0.88	10.6 q	0.93	9.8 q
25	1.67	20.7 q	1.80	20.3 q
26	3.36	56.7 q	3.40	56.8 q
27		173.5 s		172.9 s
28	4.43	48.5 d	4.41	48.5 d
29	1.40	17.5 q	1.34	17.8 q
30		176.7 s		176.6 s
31	2.12	44.7 d	2.12	45.1 d
32	1.44	29.8 t^a	1.41	29.5 t^a
33	1.85, 1.33	25.6 t^b	1.89, 1.21	25.6 t^b
34	1.81, 1.67	25.5 t	1.77, 1.66	25.5 t
35	1.85, 1.33	25.6 t^b	1.89, 1.21	25.7 t^b
36	1.44	29.0 t^a	1.41	29.7 t^a

[a-b] Assignments interchangeable.

The spectra of **1** and **2** were recorded at 600 MHz for ^1H and at 150 MHz for ^{13}C in $CDCl_3$.

The assignments were aided by ^1H-^1H COSY, DEPT, HMQC, HMBC, and NOESY.

Fig. 2. ^{1}H-^{1}H COSY, NOE and HMBC data of **1**.

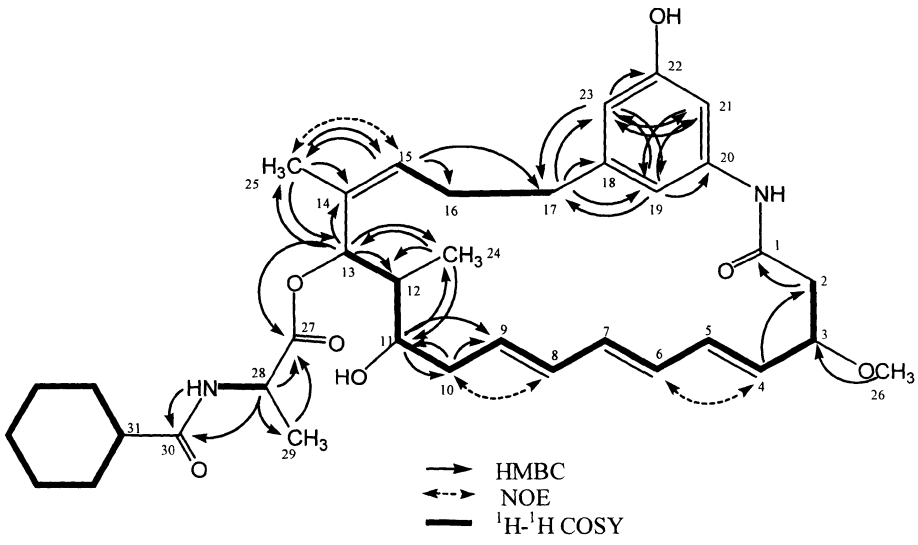

spectral data (Table 2) of **1** were very similar to those of the coisolated **2**. The ^{13}C NMR assignments (Table 2) of the coisolated **2** were established independently in this study which were in a good agreement with the reported data[18] of **2**. The ^{1}H NMR assignments (Table 2) of the coisolated **2** were first reported in this study. The major differences between **1** and **2** in ^{1}H and ^{13}C NMR data (Table 2) with HMQC data were that the methine signal (δ_H 4.93 (1H, td) and δ_C 75.5) of C-11 in **2** was upfield-shifted to δ_H 3.63 and δ_C 71.0, respectively, in **1** while the methine signal (δ_H 4.62 (1H, d) and δ_C 68.4) of C-13 in **2** was downfield-shifted to δ_H 5.92 and δ_C 75.0, respectively, in **1**. From these spectral data, it was speculated that the *N*-hexahydrobenzoylalanine moiety may be linked to C-13 in **1** instead of C-11 of **2**. The linkage position of the *N*-hexahydrobenzoylalanine moiety was determined by HMBC experiments (Fig. 2). Long range couplings were observed from the methine proton at δ_H 5.92 (H-13) to C-12, C-14, C-24, and C-25, and from the methine proton at δ_H 3.63 (H-11) to C-9, C-10, and C-24. Also, long range couplings were observed from the α-proton at δ_H 4.43 (H-28) of alanine to C-27, C-29, and C-30. The methine proton at δ_H 5.92 (H-13), not δ_H 3.63 (H-11), was long range coupled to the carbonyl carbon at δ_C 173.5 (C-27) of alanine in the *N*-hexahydrobenzoylalanine moiety. These spectral data indicated that the *N*-hexahydrobenzoylalanine moiety should be linked to C-13. The remaining structure of **1** was also confirmed by ^{1}H-^{1}H COSY, HMBC and NOESY spectral data (Fig. 2). Thus the structure of **1** was determined as shown in Fig. 1.

1 is a structural isomer of **2**, differing by the linkage position of the *N*-hexahydrobenzoylalanine side chain to the ansa moiety. **2**, a benzoid ansamycin antibiotic closely related to mycotrienins, was reported to have a potent cytocidal and cytotoxic activity[19]. The relative and absolute stereochemistry of **2** have been elucidated by chemical analysis[20].

1 and **2** exhibited the potent inhibitory effect on NO production in BV-2 microglia cells stimulated with LPS. The production of NO was assessed as the accumulation of nitrite in the culture supernatants using a coloricmetric reaction with the Griess reagent[21]. **1** and **2** inhibited dose-dependently NO production in LPS-stimulated BV-2 cells with EC_{50} (nM) values of 292.3 and 25.4, respectively as shown in Fig. 3A. This result showed that the position of the *N*-hexahydrobenzoylalanine moiety effected the activity. To see whether the observed inhibitory activity of **1** and **2** on NO production was due to a general effect on cell viability, the effect of **1** and **2** on cell viability was evaluated by MTS assay. **1** and **2** showed cytotoxic activity with IC_{50} (nM) values of 6274 and 1244, respectively, which were 21 and 49 times, respectively, higher than those of their inhibitory activity on NO production (Fig. 3B). The inhibitory activity of **1** and **2** on NO production was well separated from their cytotoxic activity, suggesting that the inhibitory activity of **1** and **2** on NO production may not be due to the loss of cell viability. The inhibitory mechanism of **1** and **2** is under investigation.

Fig. 3. The inhibitory activity on NO production (A) and the cytotoxic activity (B) of **1** and **2** in BV-2 cells.

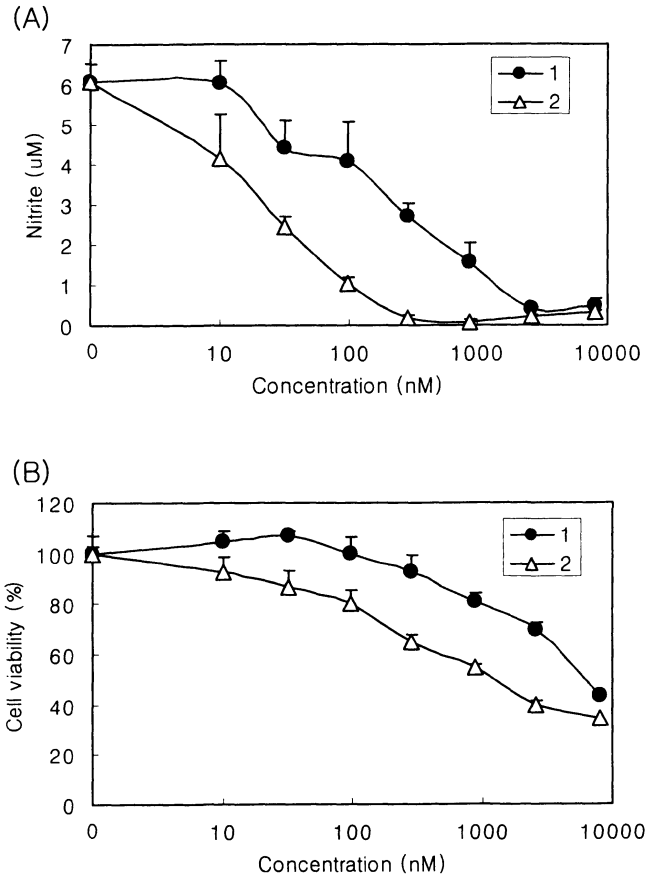

BV-2 cells were treated with vehicle (for the cytotoxic assay) or 1 μg/ml LPS (for the inhibitory assay on NO production) in the presence of the indicated concentrations of **1** and **2**. The accumulation of nitrite and cell viability were assessed 24 hours later. The data represent the mean±S.E. of three wells.

References

1) NATHAN, C. & Q. W. XIE: Maloney: Nitric oxide synthases: roles, tolls, and controls. Cell 78: 915~918, 1994
2) BREDT, D. S. & S. H. SNYDER: Nitric oxide: a physiologic messenger molecule. Annu. Rev. Biochem. 63: 175~195, 1994
3) GROSS, S. S. & M. S. WOLIN: Nitric oxide: pathophysiological mechanisms. Annu. Rev. Physiol. 57: 737~769, 1995
4) GRIFFITH, O. W. & D. J. STUEHR: Nitric oxide synthases: properties and catalytic mechanism. Annu. Rev. Physiol. 57: 707~736, 1995
5) MARLETTA, M. A.: Nitric oxide synthase: aspects concerning structure and catalysis. Cell 78: 927~930, 1994
6) NATHAN, C.: Inducible nitric oxide synthase: what difference does it make? J. Clin. Invest. 100: 2417~2423, 1997
7) AMIN, A. R. & S. B. ABRAMSON: The role of nitric oxide in articular cartilage breakdown in osteoarthritis. Curr. Opin. Rheumatol. 10: 263~268, 1988
8) BRENDAN, J. R. W.: Role of iNOS in gut inflammatory and injury. Drug News Perspect 12: 157~164, 1999
9) VODOVOTZ, Y.; M. S. LUCIA, K. C. FLANDERS, L. CHESLER, Q.-W. XIE, T. W. SMITH, J. WEIDNER, R. MUMFORD, R. WEBBER, C. NATHAN, A. B. ROBERTS, C. F. LIPPA & M. B. SPORN: Inducible nitric oxide synthase in tangle-bearing neurons of patients with Alzheimer's disease. J. Exp. Med. 184: 1425~1433, 1996
10) PARKINSON, J. F.; B. MITROVIC & J. E. MERRILL: The role of nitric oxide in multiple sclerosis. J. Mol. Med. 75: 174~186, 1997
11) GONZALEZ-SCARANO, F. & G. BALTUCH: Microglial as mediators of inflammatory and degenerative diseases. Annu. Rev. Neurosci. 22: 219~240, 1999
12) ZIELASEK, J. & H.-P. HARTUNG: Molecular mechanisms of microglial activation. Adv. Neuroimmunol. 6: 191~222, 1996
13) KIM, W.-G.; R. P. MOHNEY, B. WILSON, G.-H. JEOHN, B. LIU & J.-S. HONG: Regional difference in susceptibility to lipopolysaccharide-induced neurotoxicity in the rat brain: role of microglia. J. Neurosci. 20: 6309~6316, 2000
14) JEOHN, G.-H.; W.-G. KIM & J.-S. HONG: Time dependency of the action of nitric oxide in lipopolysaccharide-interferon-γ-induced neuronal cell death in murine primary neuron-glia cultures. Brain Research. 2000. 880(1-2): 173~177, 2000
15) HOBBS, A. J.; A. HIGGS & S. MONCADA: Inhibition of nitric oxide synthase as a potential therapeutic target. Annu. Rev. Pharmacol. Toxicol. 39: 191~220, 1999
16) CHABRIER, P-E.; C. DEMERLE-PALLARDY & M. AUGUET: Nitric oxide synthases: targets for therapeutic strategies in neurological diseases. CMLS Cell. Mol. Life Sci. 55: 1029~1035, 1999
17) ALVI, K. A.; D. D. BAKER, V. STIENECKER, M. HOSKEN & B. G. NAIR: Identification of inhibitors of inducible nitric oxide synthase from microbial extracts. J. Antibiotics 53: 496~501, 2000
18) FUNAYAMA, S.; K. OKADA, K. KOMIYAMA & I. UMEZAWA: Structure of trienomycin A, a novel cytocidal ansamycin antibiotic. J. Antibiotics 38: 1107~1109, 1985
19) FUNAYAMA, S.; K. OKADA, K. IWASAKI, K. KOMIYAMA & I. UMEZAWA: Structures of trienomycin A, B and C, novel cytocidal ansamycin antibiotics. J. Antibiotics 38: 1677~1683, 1985
20) SMITH, A. B., III; J. L. WOOD, W. WONG, A. E. GOULD, C. J. RIZZO, J. BARBOSA, K. KOMIYAMA & S. OMURA: (+)-Trienomycins A, B, C, and F and (+)-mycotrienins I and II: relative and absolute stereochemistry. J. Am. Chem. Soc. 118: 8308~8315, 1996
21) GREEN, L. C.; D. A. WAGNER, J. GLOGOWSKI, P. L. SKIPPER, J. S. WISHNOK & S. R. TANNENBAUM: Analysis of nitrate, nitrite, and [^{15}N] nitrate in biological fluids. Anal. Biochem. 126: 131~138, 1982